Title
n+p ELASTIC SCATTERING AT 3.6 GeV/c

Authors
MacNaughton, J.
Butler, W.R.
Coyne, D.G.
et al.

Publication Date
1971-06-01

Submitted to Nuclear Physics B

UCRL-20853
Preprint

C. 2

π^+p ELASTIC SCATTERING AT 3.6 GeV/c

J. MacNaughton, W. R. Butler, D. G. Coyne,
G. M. Hicks, and G. H. Trilling

June 1971

AEC Contract No. W-7405-eng-48

LAWRENCE RADIATION LABORATORY
UNIVERSITY of CALIFORNIA BERKELEY

DISCLAIMER

π^+p ELASTIC SCATTERING AT 3.6 GeV/c*

J. MacNaughton, W. R. Butler,† D. G. Coyne,‡
G. M. Hicks,† and G. H. Trilling

Department of Physics and Lawrence Radiation Laboratory
University of California, Berkeley, California 94720

June 16, 1971

Abstract: The elastic scattering of 3.6 GeV/c π^+ mesons by protons has been studied in a hydrogen bubble chamber experiment. The elastic cross section has a measured value of 7.07±0.20 mb. The forward diffraction peak has been fitted in the region $0.05 \leq -t \leq 0.6$ $(\text{GeV/c})^2$ by a form $(d\sigma/dt) = Ae^{Bt}$, where $A = 46.5 \pm 1.8$ mb/(GeV/c)^2 and $B = 6.85 \pm 0.20$ (GeV/c)$^{-2}$. From this fit and the optical theorem, the magnitude of the ratio of real to imaginary forward amplitude is 0.39±0.06, in reasonable agreement with dispersion relation calculations and simple Regge model predictions.

1. INTRODUCTION

Pion-nucleon elastic scattering has been studied extensively over a large range of momenta, with both counter and bubble chamber experiments [1]. The bubble chamber technique while often suffering from less statistical precision than electronic experiments specifically designed for studying elastic processes has the important characteristic of nearly uniform efficiency over the whole solid angle.

In this paper we report the results of a bubble chamber study of the elastic scattering of positive pions of average momentum 3.62 GeV/c by protons,

---

*Work supported by the U. S. Atomic Energy Commission.

†Now at Department of Physics, David Lipscomb College, Nashville, Tennessee.

‡Now at Department of Physics, Princeton University, Princeton, New Jersey.

based on a sample of about 10,000 events. Particular care has been exercised in the normalization of the data; consequently an accurate value of the forward cross section has been obtained which, through use of the optical theorem, permits determination of the magnitude of the real part of the forward scattering amplitude.

2. EXPERIMENTAL DETAILS

2.1. Data Handling

The data were obtained from an analysis of two-prong events in about 70,000 pictures of the LRL 72-inch hydrogen bubble chamber in a separated π^+ beam. About 25,000 pictures were at a beam momentum of 3.56 GeV/c and 45,000 at a momentum of 3.67 GeV/c. Approximately 50,000 two-prong events were measured on the LRL Flying-Spot Digitizer (FSD). First remeasurements of events which failed were also made on the FSD, and further remeasurements on the COBWEB system, consisting of measuring projectors connected on-line to an IBM 7044 computer.

Measured events were processed through the reconstruction and kinematic fitting program SIOUX and were accepted as elastic scatters if they satisfied appropriate fiducial volume and beam criteria, and satisfied the four-constraint hypothesis with a $\chi^2 \leq 23.0$. About 2% of the events dropped one constraint due to a close secondary interaction and were accepted if the three-constraint χ^2 was less than 11. With these criteria, about 10,000 elastic events were accepted.

2.2. Corrections For Systematic Scanning Loss

Events with small scattering angles and short recoil protons can easily be missed. Even those events with recoils long enough to be clearly seen may be undetected if the kink in the beam track is not seen; in such cases the recoil, though detected, may not be properly interpreted as arising from a scattering. Indeed it was experimentally found that events with recoils many centimeters in length were often missed if the scattering plane was nearly parallel to the lens axis. It is therefore not sufficient to make a cut on t, the momentum-transfer-squared, to remove scanning bias. To deal with this problem we chose to make a cut on α, the projection of the scattering angle on a plane perpendicular to the camera lens axis. From a study of the azimuth distribution of scattering with respect to the beam direction it was determined that a cutoff value of 3° for α was appropriate. Events for which $|\alpha| < 3^{\circ}$ were then removed and an appropriate correction was made. Since at 3.6 GeV/c, a 3° angle corresponds to $-t \geqq 0.04$ $(\text{GeV/c})^2$, we insured reasonably high efficiency by considering only events for which $-t \geqq 0.05$ $(\text{GeV/c})^2$. For $-t > 0.6$ $(\text{GeV/c})^2$, the above correction was not deemed necessary.

2.3. Proton Contamination Correction

The separated π^+ beam had a non-negligible proton contamination. Furthermore, at forward angles, kinematic fitting does not distinguish between proton and pion elastic scatterings. To get around this difficulty, the beam purity was monitored by including the four-constraint fit $pp \rightarrow pp\pi^+\pi^-$ among the hypotheses attempted for four-prong events. Since there is very little ambiguity between $\pi^+p \rightarrow \pi^+p\pi^+\pi^-$ and $pp \rightarrow pp\pi^+\pi^-$ this procedure provided a useful check on the contamination. A group of several rolls of film taken with either a pure proton beam or a beam containing a large fraction of incident protons were processed, treating scatterings as though they were from incident pions, and used to subtract out statistically the proton contamination using the numbers of $pp \rightarrow pp\pi^+\pi^-$ fits to provide an appropriate normalization. With this correction, the effect of proton contamination is reduced to negligible proportions.

2.4. Other Corrections

(i) Scanning Efficiency

The major difficulty, namely loss of low momentum transfer events, was already discussed, and its solution described. Since normalization was made to a total cross-section measurement from counter experiments it was of some importance to compare the scanning efficiency for elastic scatterings with $-t > 0.06\ (\mathrm{GeV}/c)^2$ and $\alpha \geq 3^\circ$ with that for other event topologies. From a rescan of 10% of the sample the scanning efficiency was found to be 98% with no difference between topologies. A 2% contribution to the error in the cross section has been folded in to take account of possible differential scanning inefficiency.

(ii) Unresolved Events

Approximately 4% of the events were, after completion of measurements, neither accepted nor rejected, principally because of some measurement failure. It turned out that nearly all such events could be classified as elastic or inelastic after careful inspection of all available measurement information. These events, therefore, made no significant contribution to the final cross-section error.

3. RESULTS

3.1. Elastic Cross Section

Since no significant differences were found between the results of 3.56 and 3.67 GeV/c, we have combined them for purposes of analysis. As discussed further on, a fit of the form Ae^{Bt} was made to the t distribution. The values of A, B were then used to calculate the number of events between $-t = 0$ and $-t = 0.05\ (\mathrm{GeV}/c)^2$ excluded by the criteria discussed earlier. The corrected number of elastic scatterings was then compared to the corrected total number of π^+p interactions found. The result is

$$\frac{\sigma_{\text{elastic}}}{\sigma_{\text{total}}} = 0.251 \pm 0.007$$

where the roughly equal error contributions are from (a) statistics, (b) an assumed 2% error in differential scanning efficiency.

From the known total cross section at 3.62 GeV/c, $\sigma_{\text{total}} = 28.18 \pm 0.015$ mb [2], we determine the elastic cross section

$$\sigma_{\text{elastic}} = 7.07 \pm 0.20 \text{ mb} \quad .$$

3.2. Angular Distribution

The complete differential cross section is given in table 1 and fig. 1. More detailed representations of the forward and backward parts are shown in figs. 2 and 3. The data are in good agreement with the results of Coffin et al. [3]. Several of the interesting features such as the backward peak and dip structure just ahead of it have been studied with much greater statistical precision in spark chamber experiments specifically designed for that purpose [4], and we do not discuss them in detail here except to note that within the limited statistics our data are in agreement with these other much more precise experiments. We concentrate our detailed analysis on the forward diffraction peak where statistics are relatively plentiful, and where our sensitivity at low momentum transfers as well as the minimal systematic uncertainties inherent in the bubble chamber technique make the data of particular interest.

3.3. Forward Diffraction Peak

The forward angular distribution is shown in detail in fig. 2. A fit of the form

$$\left(\frac{d\sigma}{dt}\right) = \left(\frac{d\sigma}{dt}\right)_0 e^{Bt} \qquad (1)$$

gives a good representation of the data between $-t = 0.05$ and $-t = 0.60$ $(\text{GeV}/c)^2$ with the parameters

$$\left(\frac{d\sigma}{dt}\right)_o = 46.5\pm1.8 \text{ mb/(GeV/c)}^2$$

$$B = 6.85\pm0.20 \text{ (GeV/c)}^{-2} \quad .$$

The quoted uncertainty in $(d\sigma/dt)$ is believed to represent realistically both the statistical and the systematic errors. The contribution to $(d\sigma/dt)_o$ from the imaginary part of the forward amplitude, as determined from the optical theorem, is 40.2 mb/(GeV/c)^2. The contribution of the real part of the forward amplitude is then 6.3±1.8 mb/(GeV/c)^2 from which one easily finds that the ratio a_+ of real to imaginary part of the forward π^+p amplitude has the magnitude

$$|a_+| = 0.39\pm0.06 \quad .$$

This figure is to be compared with the following theoretical predictions: (i) Dispersion relation calculations predict the value of $a_+ \approx -0.3$ [5]. (ii) A simple Regge pole model incorporating only P,P' and ρ exchanges with Regge intercepts $\alpha_\rho(0) = \alpha_{P'}(0) = 1/2$, $\alpha_P(0) = 1$ would predict for the ratios a_+ and a_-

$$a_\pm = \frac{\sigma_\infty - \sigma_\mp}{\sigma_\pm} \tag{2}$$

where $\sigma_\pm$ is the $\pi^\pm p$ total cross section and σ_∞ is the asymptotic limit of the total πp cross section. Using $\sigma_+ = 28.2$ mb, $\sigma_- = 31.3$ mb [2] and estimating $\sigma_\infty = 21$ mb, a_+ is predicted to be -0.40. Our experimental value of $|a_+|$ is in good agreement with these predictions.

It is useful to note that a measurement of a_+ can be combined with the forward charge exchange cross section $(d\sigma/dt)_o^{ce}$ to obtain the value of a_-, the ratio of real to imaginary parts of the forward π^-p scattering amplitude:

$$a_- = \frac{a_+\sigma_+}{\sigma_-} + \frac{\sqrt{2(d\sigma/dt)_o^{ce} - (\sigma_- - \sigma_+)^2}}{\sigma_-} \quad . \tag{3}$$

In choosing the sign in front of the discriminant we have taken a_+ negative as predicted by theory and assumed a positive ratio for real to imaginary parts of the charge exchange amplitude, as expected if ρ exchange dominates that process.

The value of $(d\sigma/dt)^{ce}$ has been measured at 3.67 GeV/c by Sonderegger et al. [6]. In the momentum transfer range 0 to -0.05 $(GeV/c)^2$ they find $(d\sigma/dt)^{ce} = 750 \pm 40\ \mu b/(GeV/c)^2$. We take for the calculation of a_-, $(d\sigma/dt)_o^{ce} = 750 \pm 100\ \mu b/(GeV/c)^2$ where the increased error reflects the uncertainty of the actual value in the forward direction. From formula (3) we find,

$$a_- = -\ 0.21 \pm 0.056\ .$$

Again we compare with theoretical expectations. Dispersion relations give $a_- = -\ 0.18$, whereas the Regge model described above would give $a_- = -\ 0.23$. Agreement with experiment is thus excellent.

We express our thanks to our scanning and measuring staff and to the Data Handling Group under Howard White.

REFERENCES

[1] See, for example, G. Giacomelli, P. Pini, and S. Stagni, A Compilation of Pion-Nucleon Scattering Data, CERN/HERA 69-1.

[2] A. Citron, W. Galbraith, T. F. Kycia, B. A. Leontic, R. H. Phillips, A. Rousset and P. H. Sharp, Phys. Rev. 144 (1966) 1101.

[3] C. T. Coffin, N. Dikmen, L. Ettlinger, D. Meyer, A. Saulys, K. Terwilliger, and D. Williams, Phys. Rev. 159 (1967) 1169.

[4] B. B. Brabson, R. R. Crittenden, R. M. Heinz, R. C. Kammerud, H. A. Neal, H. W. Paik, and R. A. Sidwell, Phys. Rev. Letters 25 (1970) 553; R. A. Sidwell, R. R. Crittenden, K. F. Galloway, R. M. Heinz, and H. A. Neal, Phys. Rev. D3 (1971) 1523.

[5] V. S. Barashenkov, Physics Letters 19 (1965) 699.

[6] P. Sonderegger, J. Kirz, O. Guisan, P. Falk-Vairant, C. Bruneton, P. Bargeaud, A. V. Stirling, C. Caverzasio, J. P. Guillaud, M. Yvert, and B. Amblard, Physics Letters 20 (1966) 75.

Table 1. Differential cross section, $d\sigma/dt$, for π^+p elastic scattering at 3.63 GeV/c

|t| interval $(GeV/c)^2$	$d\sigma/dt$ $mb/(GeV/c)^2$	|t| interval $(GeV/c)^2$	$d\sigma/dt$ $\mu b/(GeV/c)^2$
0.05-0.10	27.76±1.05	1.5-1.6	148±36
0.10-0.15	18.78±0.75	1.6-1.7	121±30
0.15-0.20	14.62±0.61	1.7-1.8	60±20
0.20-0.25	9.23±0.49	1.8-1.9	47±18
0.25-0.30	7.56±0.42	1.9-2.0	60±20
0.30-0.35	5.45±0.35	2.0-2.1	54±19
0.35-0.40	3.57±0.28	2.1-2.4	20^{+6}_{-5}
0.40-0.45	2.78±0.23	2.4-2.7	12^{+5}_{-4}
0.45-0.50	1.81±0.20	2.7-3.0	6^{+4}_{-2}
0.50-0.55	1.68±0.17	3.0-3.3	$3^{+3}_{-1.5}$
0.55-0.60	0.91±0.13	3.3-3.6	$5^{+3.5}_{-2}$
0.6-0.7	0.89±0.08	3.6-3.9	9^{+5}_{-3}
0.7-0.8	0.46±0.06	3.9-4.2	12^{+5}_{-4}
0.8-0.9	0.376±0.052	4.2-4.5	11^{+5}_{-3}
0.9-1.0	0.302±0.048	4.5-4.8	15^{+6}_{-4}
1.0-1.1	0.181±0.038	4.8-5.1	35^{+8}_{-7}
1.1-1.2	0.289±0.047	5.1-5.4	28^{+7}_{-6}
1.2-1.3	0.235±0.041	5.4-5.7	34^{+8}_{-7}
1.3-1.4	0.154±0.032	5.7-6.0	18^{+6}_{-5}
1.4-1.5	0.168±0.038	6.0-6.05	92^{+34}_{-25}

FIGURE CAPTIONS

Fig. 1. Differential cross section, $d\sigma/dt$, for π^+p elastic scattering at 3.63 GeV/c.

Fig. 2. Differential cross section in the momentum transfer region $0.05 \leq -t \leq 0.8$ $(\mathrm{GeV}/c)^2$. The solid line segment indicates the extrapolation to $t = 0$.

Fig. 3. Differential cross section, $d\sigma/du$, near the backward direction.

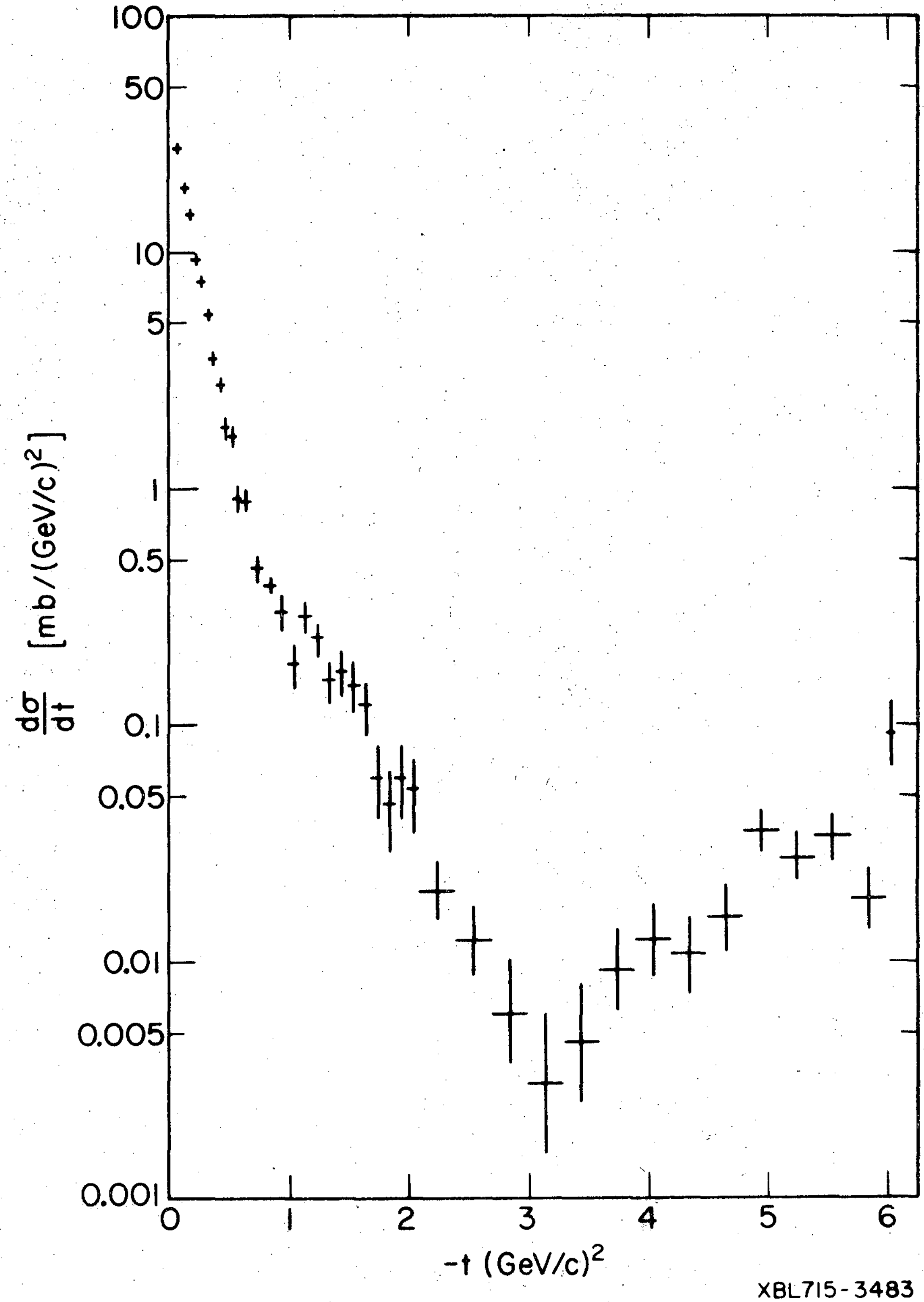
100
50
10
5
1
0.5
0.1
0.05
0.01
0.005
0.001
0
1
2
3
4
5
6
dσ/dt [mb/(GeV/c)²]
-t (GeV/c)²
XBL715-3483

Fig. 1

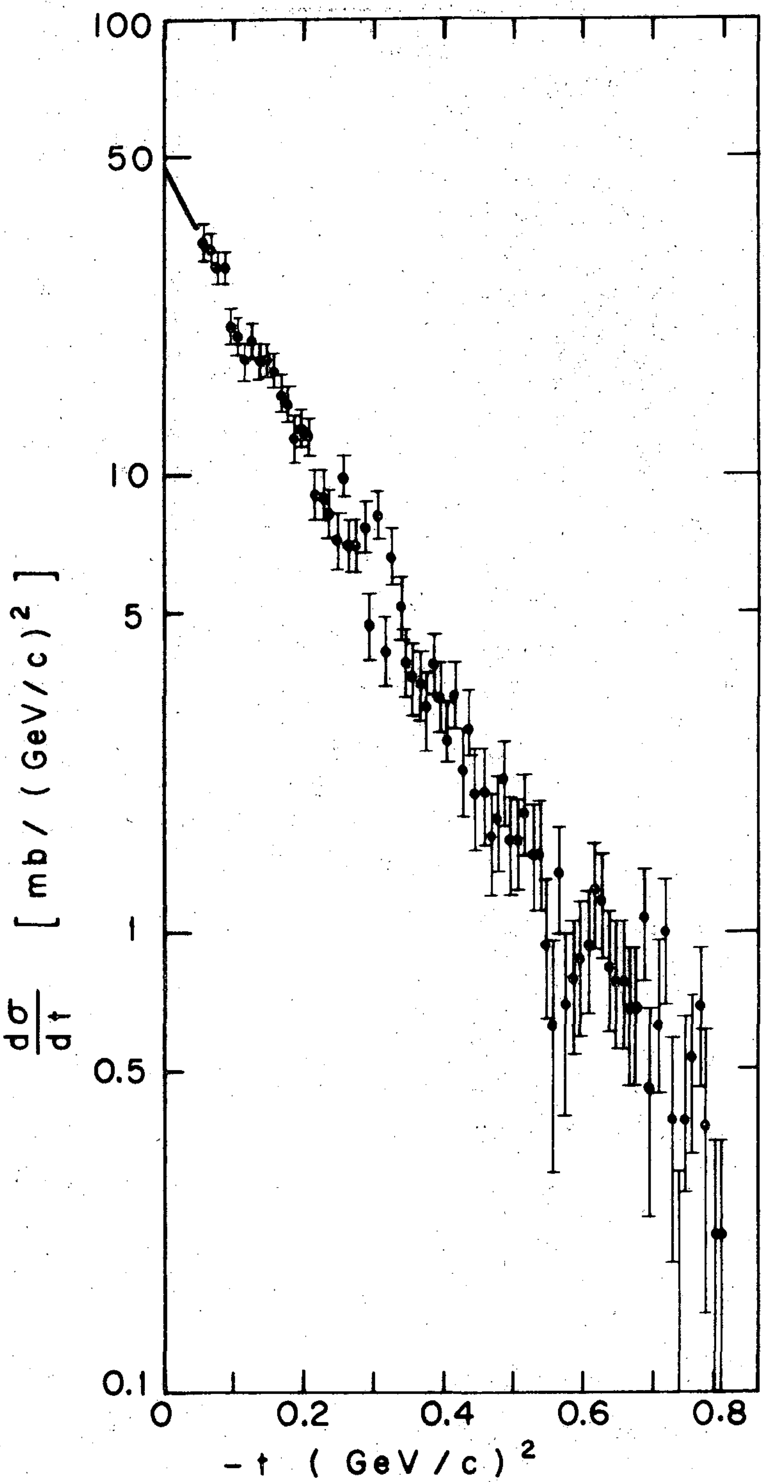

XBL715-3443

Fig. 2

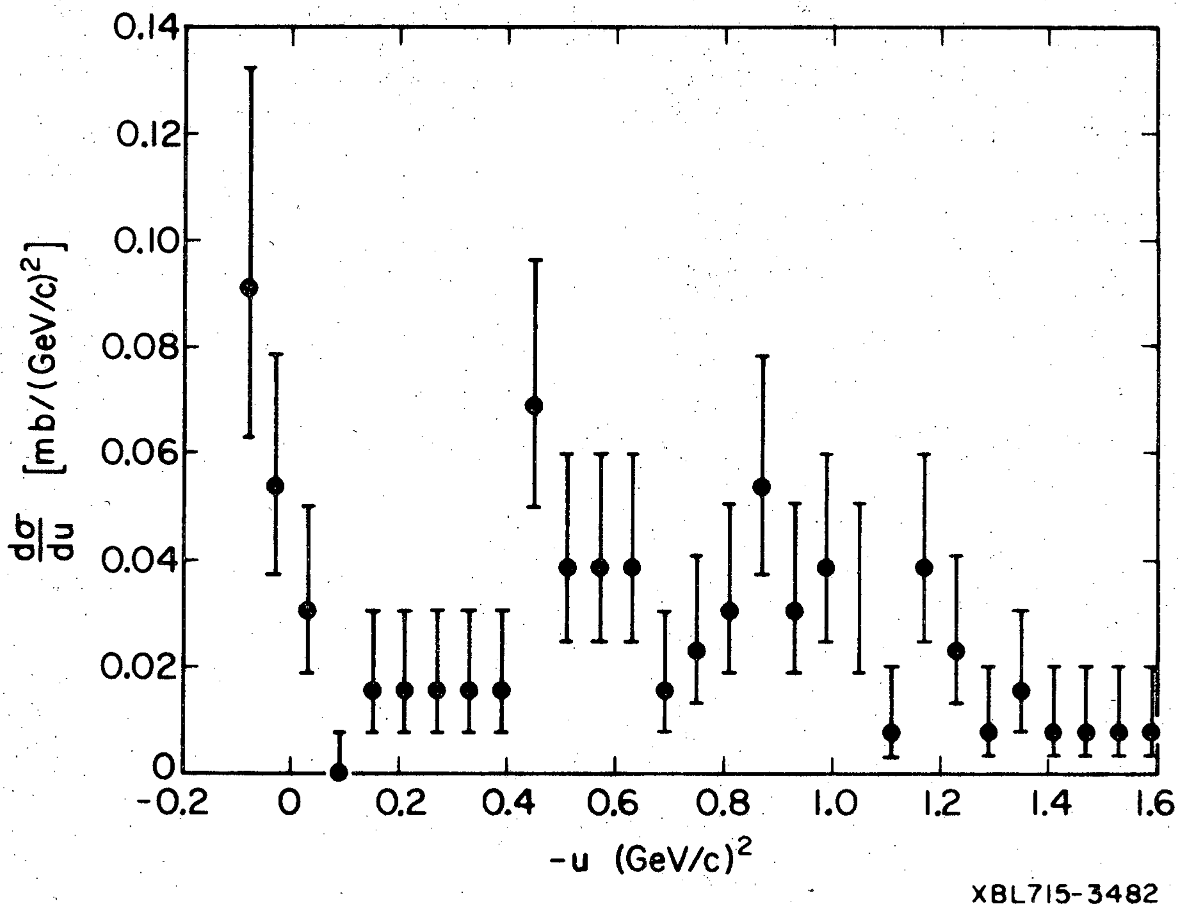
0.14
0.12
0.10
0.08
0.06
0.04
0.02
0
$\frac{d\sigma}{du}$ [mb/(GeV/c)^2]
-0.2
0
0.2
0.4
0.6
0.8
1.0
1.2
1.4
1.6
-u (GeV/c)^2
XBL715-3482

Fig. 3

TECHNICAL INFORMATION DIVISION
LAWRENCE RADIATION LABORATORY
UNIVERSITY OF CALIFORNIA
BERKELEY, CALIFORNIA 94720